

Nanotechnology Advances in Targeted Drug Delivery Systems

Professor Costas Kiparissides

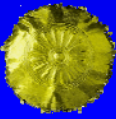
*Department of Chemical Engineering, Aristotle University of Thessaloniki &
Center for Research and Technology Hellas (CERTH)*

INNOVATION, RECHERCHE ET ENTREPRENARIAT
ENERGIE, BIOTECHNOLOGIE, ENVIRONNEMENT, SANTE

October 9, Thessaloniki, Greece



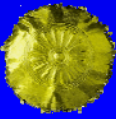
Outline



- Nanomedicine
- Controlled Drug Delivery Systems
- Development of Novel Nanocarriers
- Respiratory Delivery
- Future Challenges



Nanomedicine



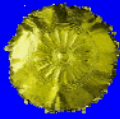
The term **Nanomedicine** refers to the application of nanotechnology to **diagnosis and treatment** of diseases.

- ✓ It deals with the interactions of **nanomaterials** (surfaces, particles, etc.) or analytical **nanodevices** with “living” **human material** (cells, tissue, body fluids).
- ✓ It is an extremely large field ranging from in vivo and in vitro **diagnostics to therapy** including **targeted delivery and regenerative medicine**.





Drug Delivery Systems

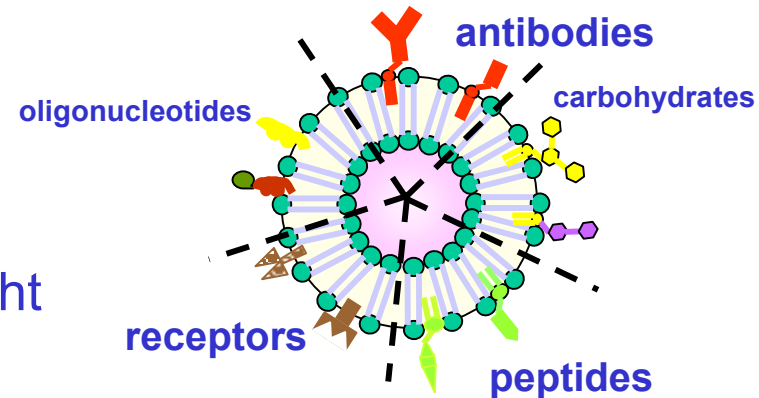


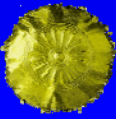
The concept of “Clever” drug targeting system includes the coordinating behavior of three components: **the targeting moiety, the carrier and the therapeutic drug.**

- The first one recognizes and binds the target.
- The second one carries the drug
- The third one provides a therapeutic action to the specific site

Targeting moieties:

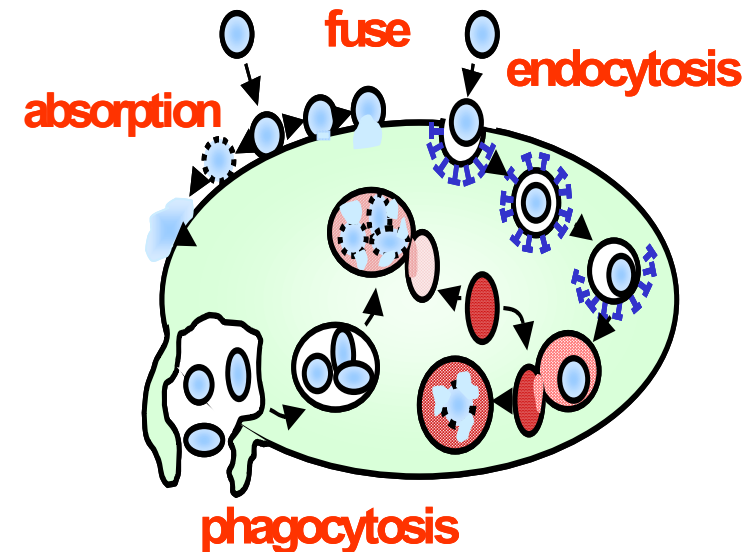
- Antibodies
- Proteins
- Lipoproteins
- Hormones
- Charged molecules
- Polysaccharides
- Low-molecular-weight ligands

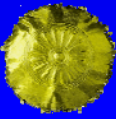




The potential of targeted delivery will only be realized with a much better understanding of **how such structures interact with the body and its components – in vitro and in vivo.**

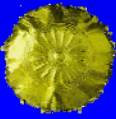
- ✓ **Interaction of nanostructures with plasma proteins** and relation between protein adsorption and removal of nanostructures from the circulation by the reticulo-endothelial system.
- ✓ **Adsorption of nanostructures to cells** (in relation to the surface chemical characteristics, size and shape of the nanostructures).
- ✓ **Uptake and recycling, trans-endocytosis and endosomal escape** of nanostructures.
- ✓ **Safety evaluation:** In vitro/in vivo cytotoxicity, haemocompatibility, immunogenicity and genotoxicity testing.
- ✓ In vivo carrier **biodistribution and degradation.**





➤ The potential of nanocarriers as Drug Delivery Systems

- ✓ Exhibit higher intracellular uptake
- ✓ Can penetrate the submucosal layers while the microcarriers are predominantly localized on the epithelial lining.
- ✓ Can be administered into systemic circulation without the problems of particle aggregation or blockage of fine blood capillaries.
- ✓ The development of targeted delivery is firmly built on extensive experience in pharmaco-chemistry, pharmacology, toxicology, and nowadays is being pursued as a multi- and interdisciplinary effort.

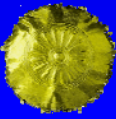


Nano BioPharmaceutics

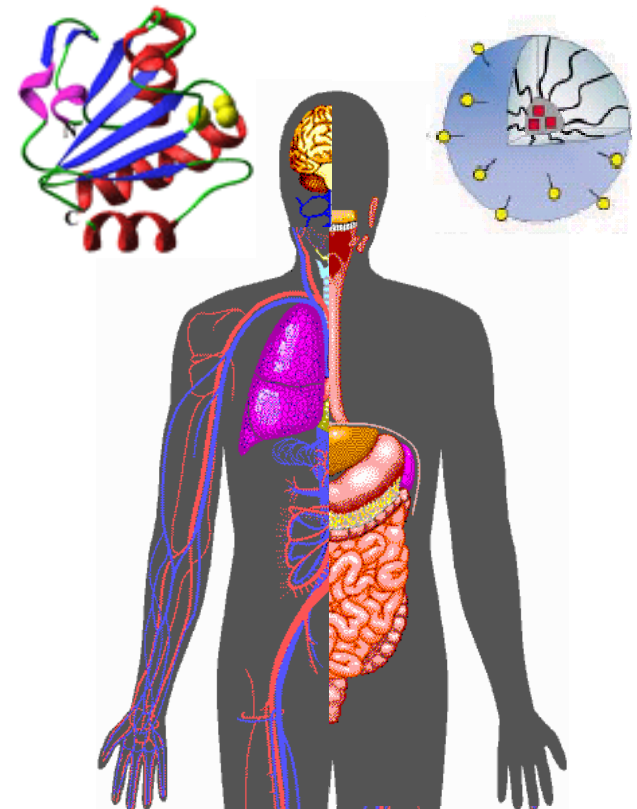
Nanoscale Functionalities for
Targeted Delivery of Biopharmaceutics



Our Mission

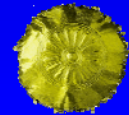


- “NanoBioPharmaceutics” aims at breakthrough advances in novel biopharmaceutics delivery systems for the treatment of diabetes, cancer, AIDS, Alzheimer’s disease, and other neurodegenerative diseases.
- Nanocarrier-based protein/peptide (P/P) delivery systems for respiratory and oral delivery and blood brain barrier (BBB) crossing applications are developed within this project allowing a targeted and controlled release of the drugs.

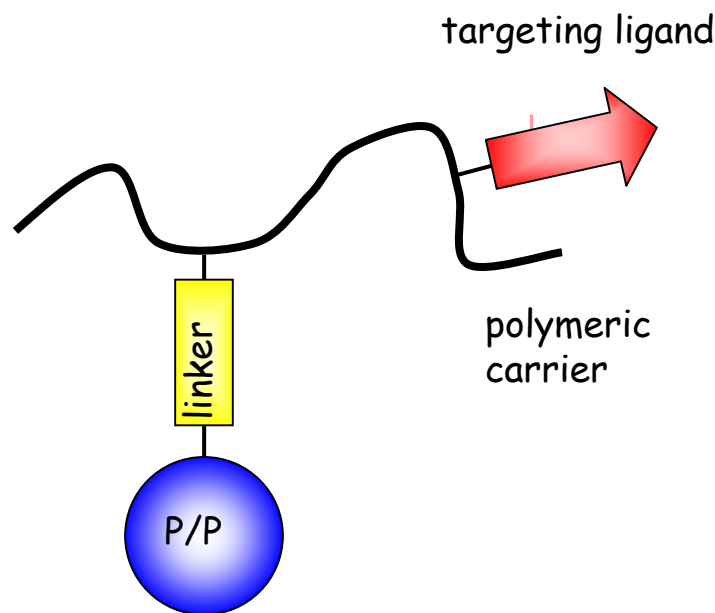




Polymer- P/P Drug Complexes



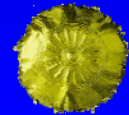
- Covalent attachment of P/P Drugs to polymer chains via specific linkers.



- | | |
|--------------------|--|
| • P/P | : peptide / protein |
| • Linker | : enzymatically or pH sensitive |
| • Targeting ligand | : peptide / saccharide |
| • Polymer carrier | : Hydrophilic polymers, polyelectrolytes |

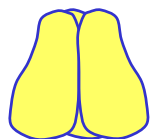


PEGylated TNF-alpha (PEG-TNF)



PEG-TNF for Cancer Therapy

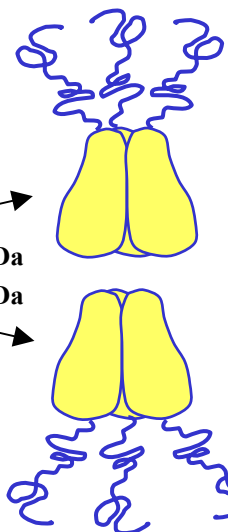
Cys-analogs for site-specific pegylation



PEGylation at the tip of the trimer

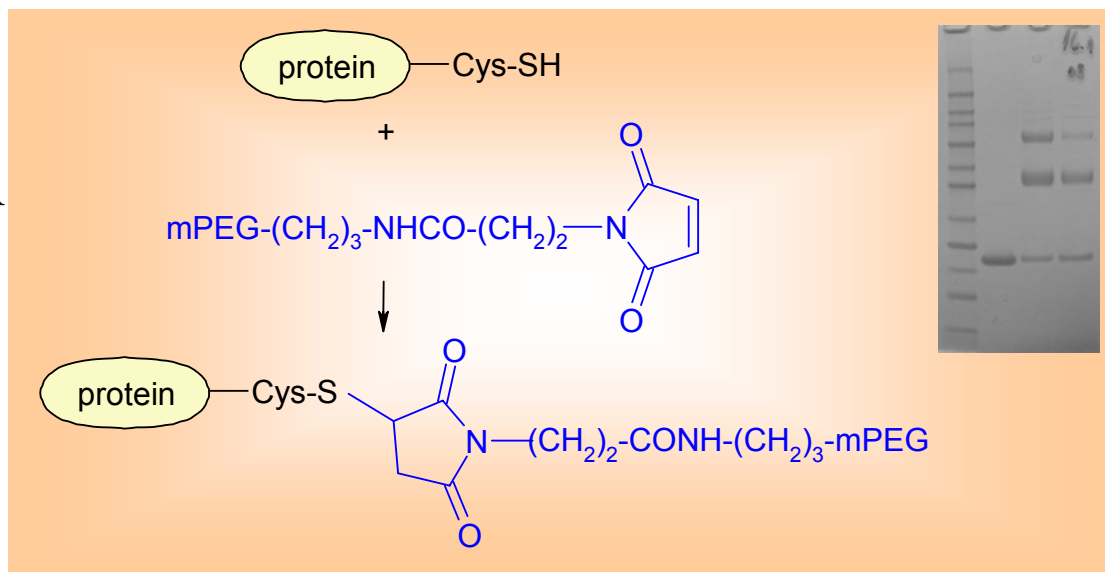
3 x 10 kDa
3 x 20 kDa

PEGylation at the base of the trimer opposite to the tip



•A

•B

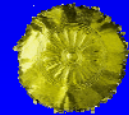


Goals:

- ✓ Prolonged half-life (30 min → 5 – 10 hrs)
- ✓ Reduced toxicity
- ✓ Better protection to degradation
- ✓ Improved antitumor activity



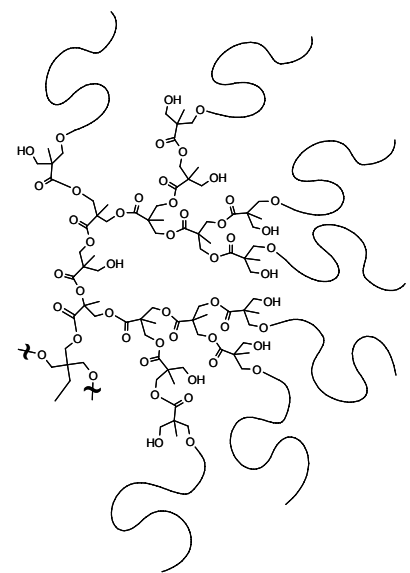
Dendritic Polymers



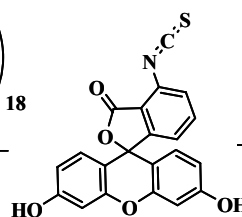
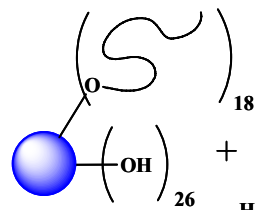
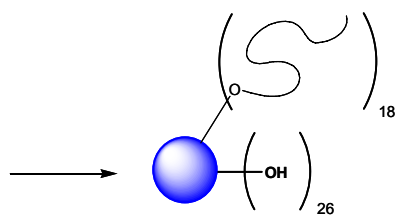
➤ Multifunctional **dendrimers** and **hyperbranched polymers** as DDS.

- ✓ Cell specificity via attachment of targeting ligands.
- ✓ Decreased toxicity, biocompatibility, stability, and protection in the biological milieu via functionalization with PEG.

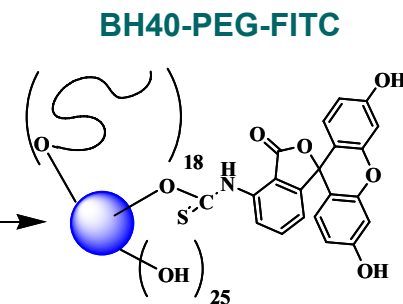
FITC-labeled PEGylated biodegradable hyperbranched polyester as a carrier for ADNF peptide



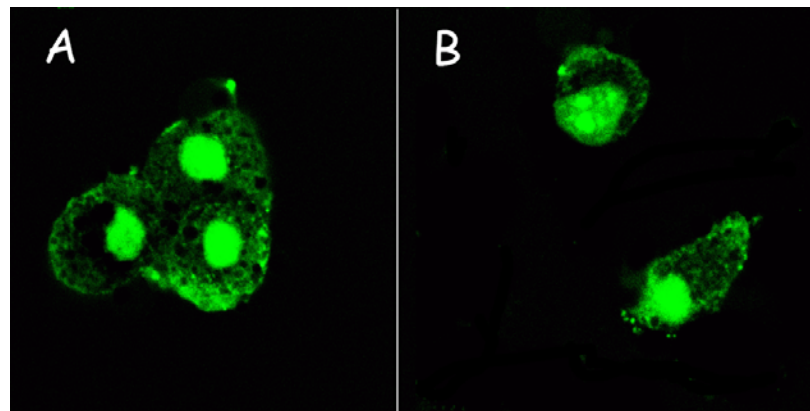
PEGylated BOLTORN H40



24h, rt
TBTL

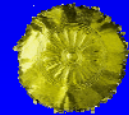


Confocal microscopy on A549 cells revealed preferential uptake of BH40-PEG in cells nuclei



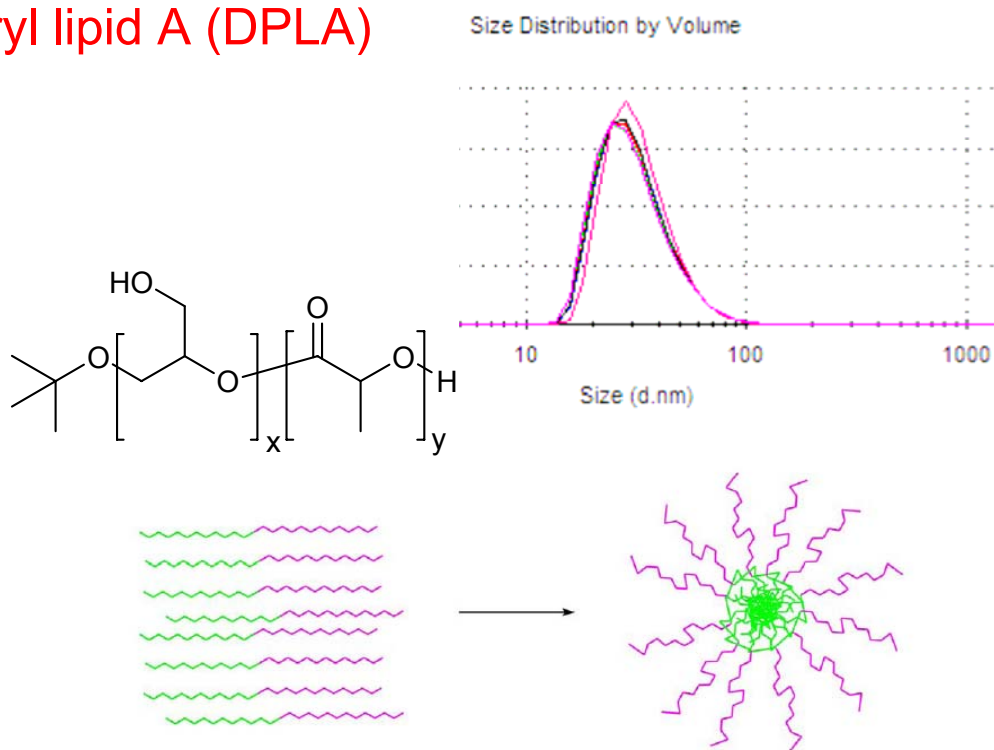


Block Copolymer Micelles

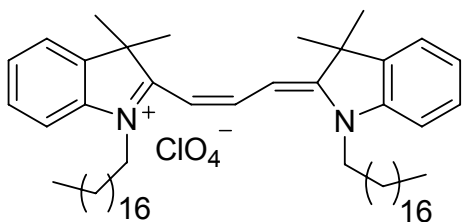


Poly(glycidol)-block-poly(lactide) NPs loaded with ovalbumin (OVA) and diphosphoryl lipid A (DPLA)

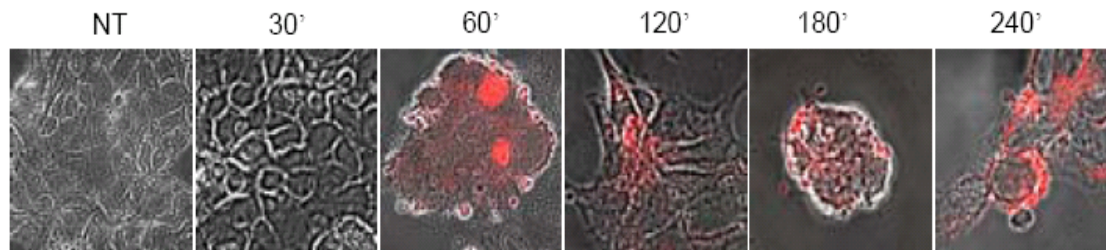
- ✓ Mean size: ~30nm
- ✓ Zeta potential: -19.1 ± 16.8 mV
- ✓ OVA loading: up to 10%wt
- ✓ DPLA loading: up to 5%wt
- ✓ Labelling: 1,1'-dioctadecyl-3,3,3',3'-tetramethylindocarbocyanine perchlorate (Dil)
- ✓ NPs are stable following 7 days incubation in water



Dil



MW 7000
(18 nm)

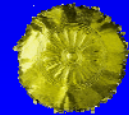


37°C

Caco-2 cells treated with NPs labelled with Dil

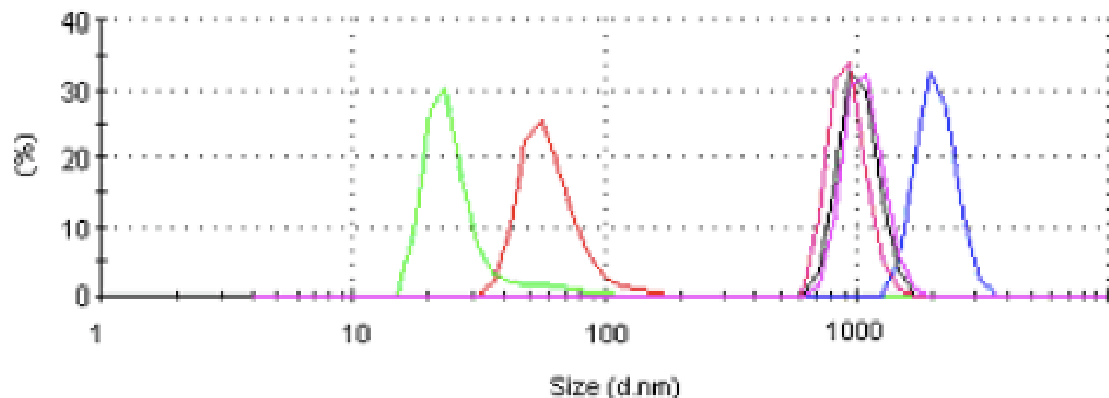


Nanogels

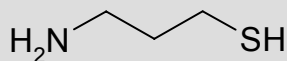


➤ Three-dimensional, hydrophilic, stimuli-responsive polymeric networks: exhibit dramatic changes in network structure or swelling behavior in response to various external stimuli.

- ✓ Thermosensitive: NIPAAm-Aam, NIPAAm-DMAM, DEAM-DMAM
- ✓ pH sensitive: 2-hydroxyethyl methacrylate, acrylic acid

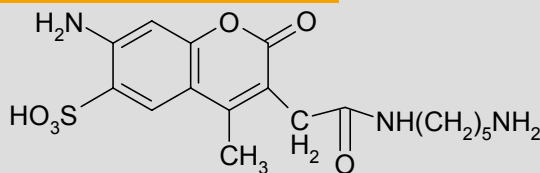


Adhesion



Cysteamine hydrochloride

Fluorescence



Alexa fluor 350 cadaverine

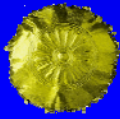
Surface modification

- 25°C
- 35°C
- 39°C
- 41°C
- 46°C
- 50°C



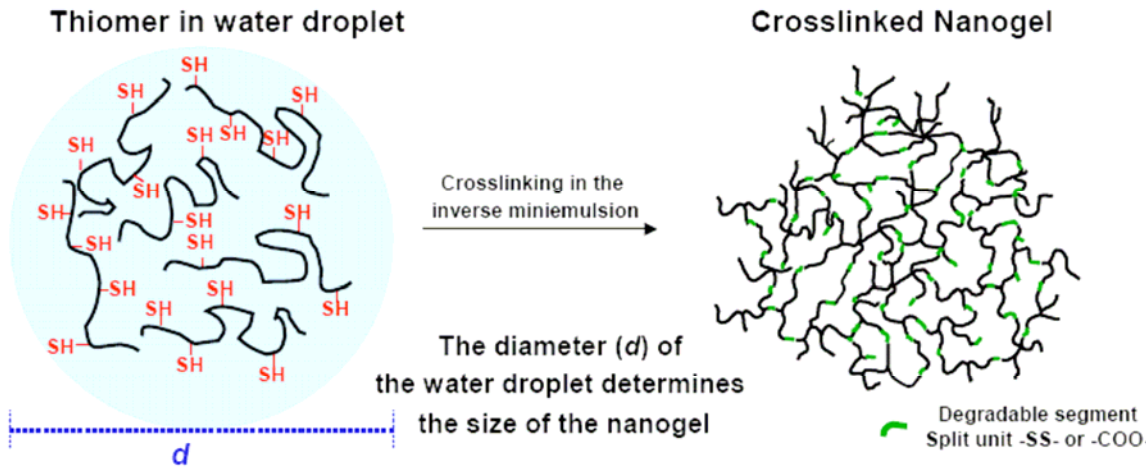


Thiomer Nanogels



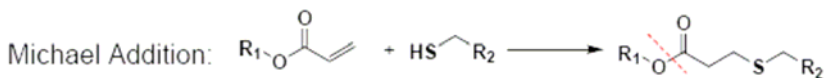
➤ Biodegradable nanogels by crosslinking thiol functionalized starPEG or poly(glycidols) in the inverse miniemulsion via oxidation or Michael addition with diacrylates.

- ✓ Synthesis of hydrophilic oligomers via radical polymerization with cysteamine-modified N-acrylosuccinimide.
- ✓ Crosslinking of hydrophilic polymers possessing hydroxyl groups with disulfide crosslinker.

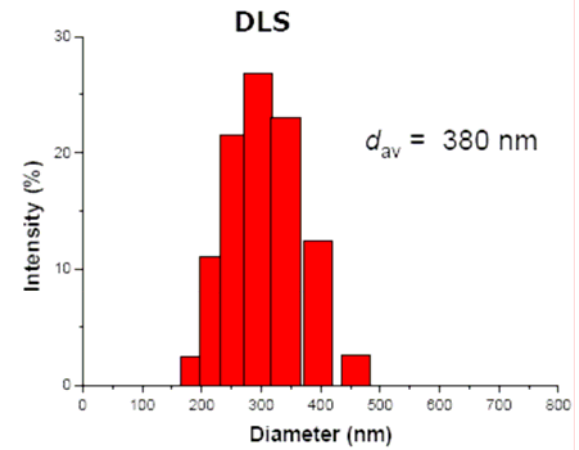


Crosslinking of -SH groups:

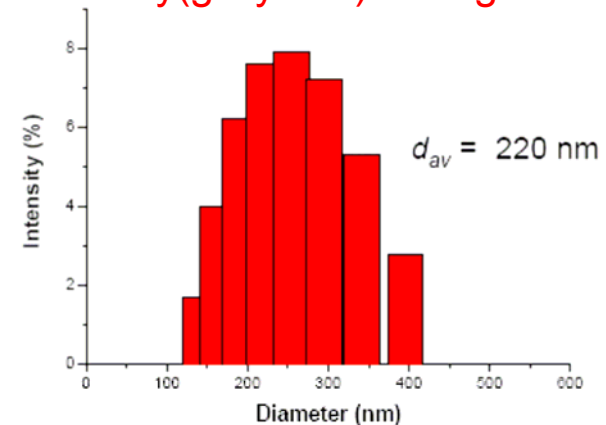
Oxidation: $-SH + HS- \rightleftharpoons -SS-$



starPEG nanogels

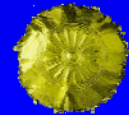


Poly(glycidols) nanogels

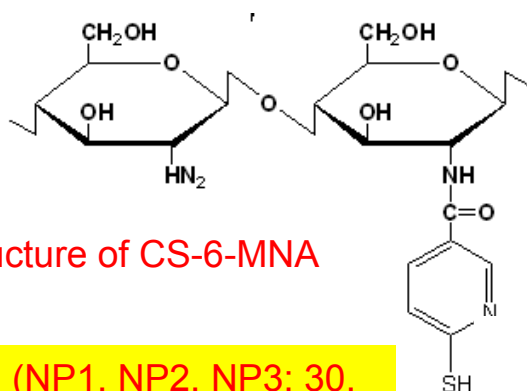
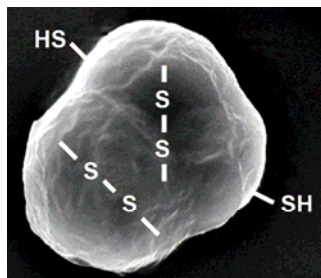




Chitosan



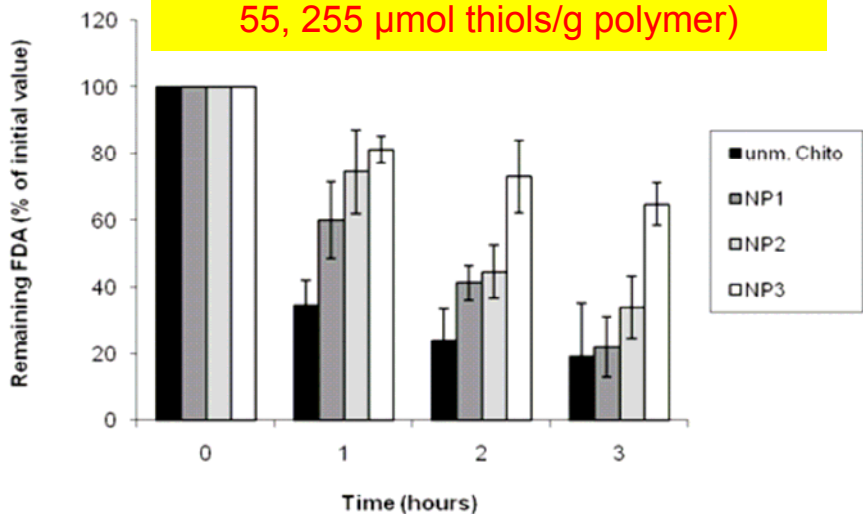
- Synthesis of **chitosan-6 mercapto-nicotinic acid (CS-6-MNA)** via a carbodiimide mediated reaction.
- Preparation of NPs with CS-6-MNA and unmodified CS by ionic gelation.



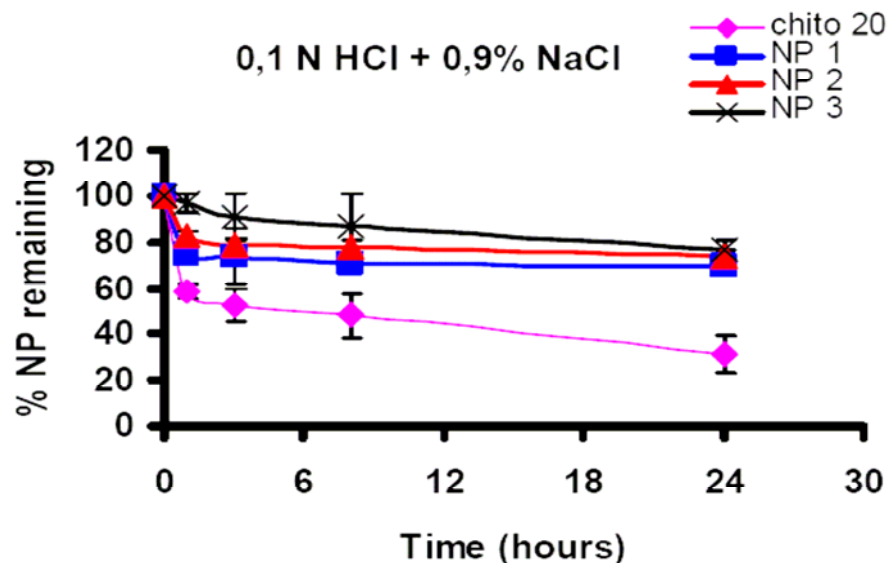
Structure of CS-6-MNA

- ✓ Size: 250nm
- ✓ Zeta potential: 10-20mV
- ✓ Very high mucoadhesion (> 70 fold improvement over non thiolated polymer)
- ✓ Very strong and rapid in situ gelling properties

Mucoadhesion (NP1, NP2, NP3: 30, 55, 255 μmol thiols/polymer)

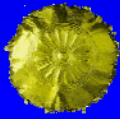


Particle stability

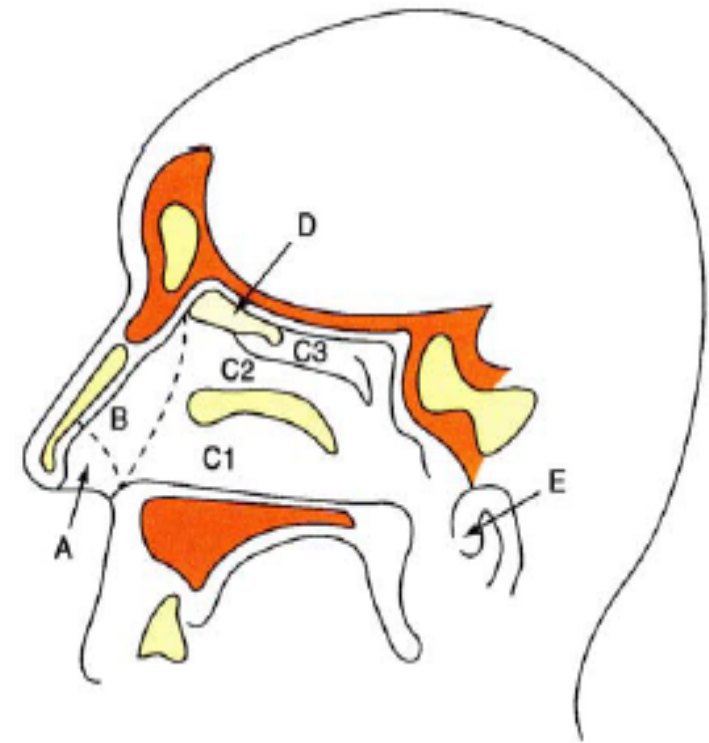




Nasal Vaccination



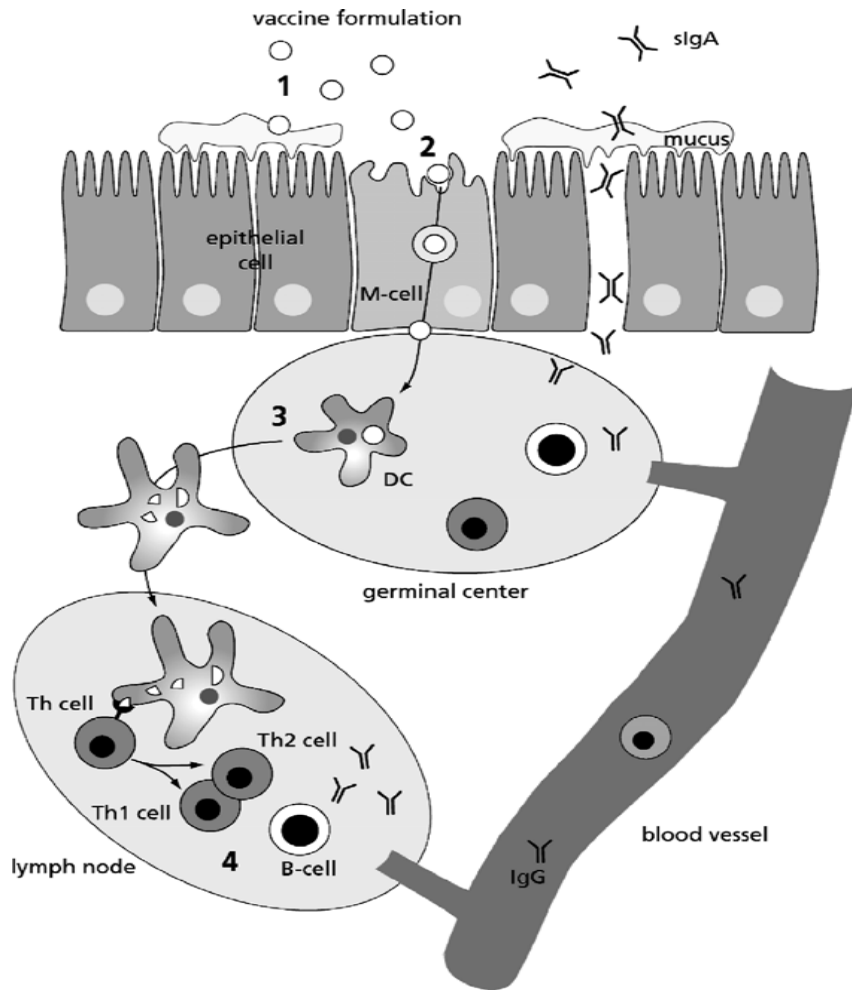
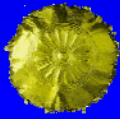
- **Vaccination** is the most effective way of fighting infectious diseases like HIV, malaria, influenza, etc.
- Among the potential **needle-free routes**, nasal vaccination is particularly attractive.
- The nose is **easily accessible** (i.e., administration via **drops or sprays**) and the nasal cavity is equipped with a **high density of dendritic cells (DC)** that can mediate **strong systemic and local immune responses** against pathogens that invade the human body through the respiratory tract.



Sagittal section of human nasal cavity



A Roadmap to Successful Nasal Vaccine Delivery

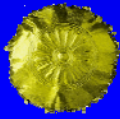


1. Prolonging the nasal residence time (mucoadhesion).
2. M-cell targeting (antigen uptake by M-cell transport).
3. Delivery to and subsequent activation/maturation of dendritic cells (DC).
4. Induction of cytotoxic T-lymphocyte immune responses.

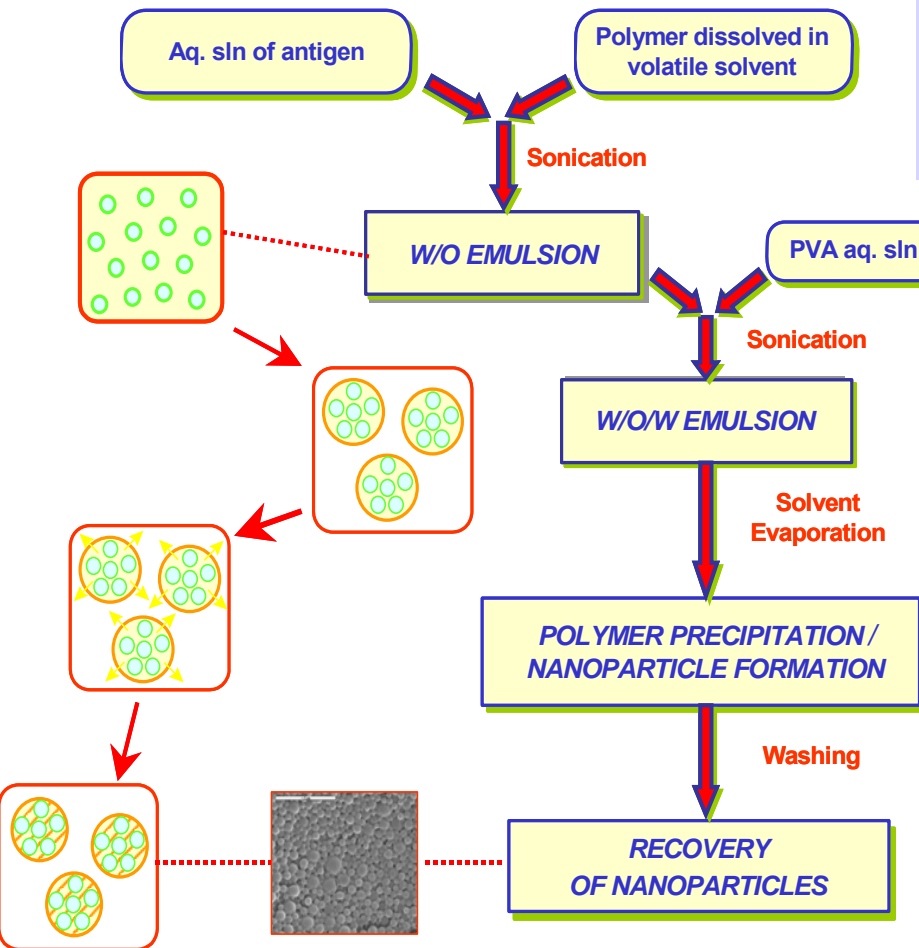
Three major elements should constitute the nanostructure-based vaccines: the carrier, the antigen and the adjuvant (e.g., MPLA, CpG, etc.)



Particle Synthesis



Synthesis of PLGA NPs by the Double Emulsion Method



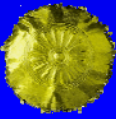
- PLGA: Resomer RG752H
- Antigen: Profos AG EndoGrade™ Ovalbumin, <1EU/mg
- Adjuvant: Monophosphoryl lipid A (MPLA)

- ✓ Various OVA and MPLA initial concentrations (0.15-10mg OVA, 200 μg – 2 mg MPLA)
- ✓ BSA-FITC loaded PLGA NPs for cell uptake studies
- ✓ OVA loaded and blank PLGA NPs as controls.

Synthesized amount per batch: ~ 60mg



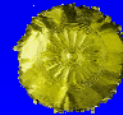
Characterization



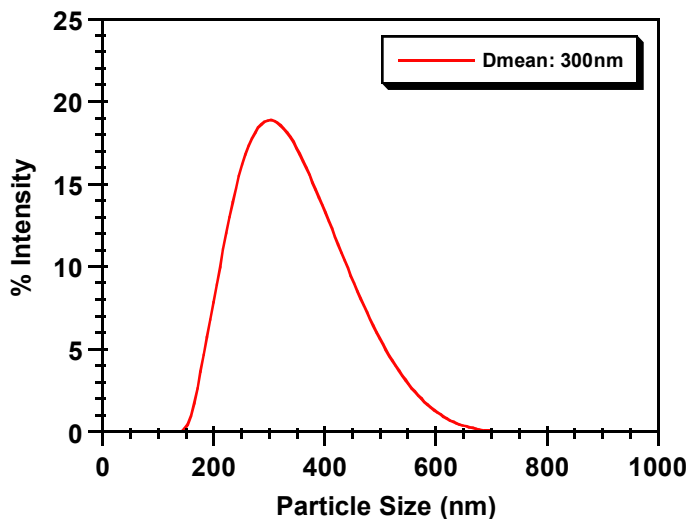
- ✓ Surface morphology: SEM
- ✓ Particle size distribution: DLS
- ✓ Zeta potential: Aqueous electrophoresis measurements
- ✓ OVA & BSA-FITC loading: Bicinchoninic acid (BCA) protein assay
- ✓ MPLA loading: Limulus Amebocyte Lysate (LAL) kit
- ✓ WGA-FITC Quantification: UV (490nm)
- ✓ OVA integrity: Gel electrophoresis
- ✓ Cytotoxicity: MTS, LDH assays (*School of Biology, AUTh*)
- ✓ Endotoxicity: LAL & E-selectin induction (*JGU*)
- ✓ Haemocompatibility (*ULG*)
- ✓ Cell uptake: Confocal microscopy (*Institut Pasteur*)



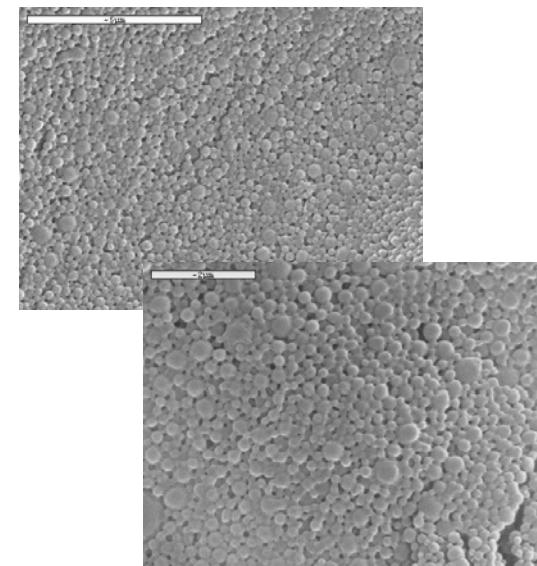
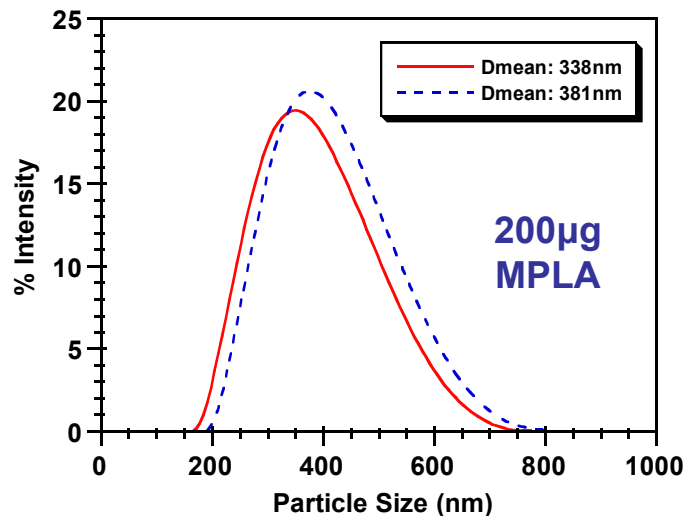
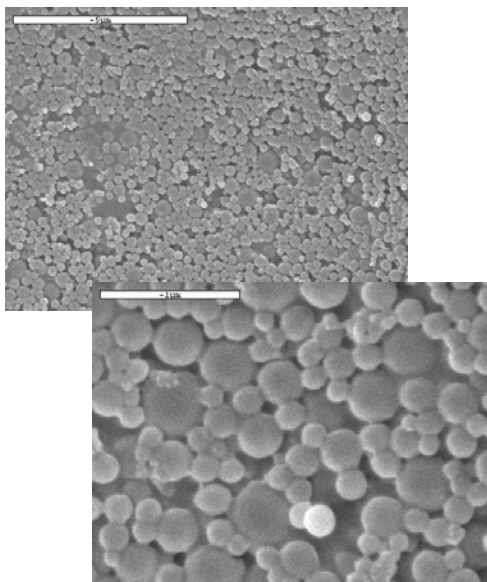
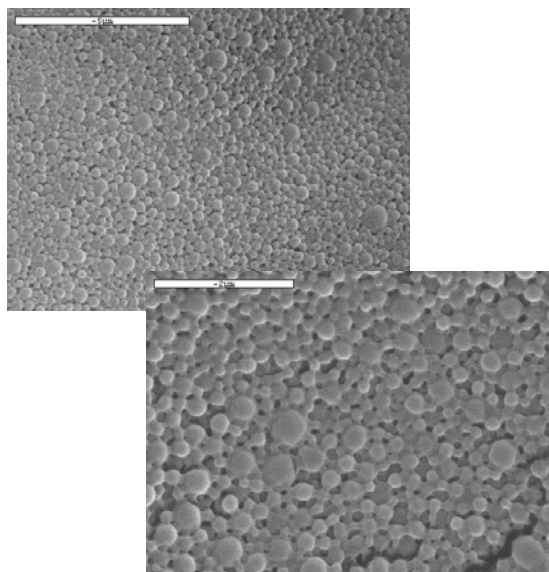
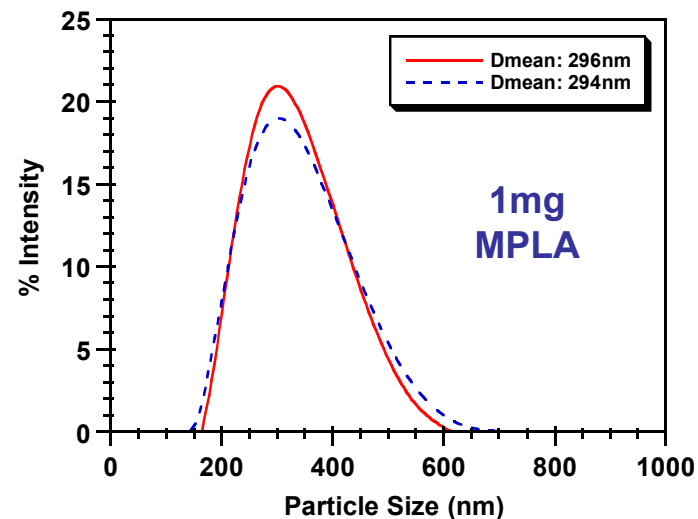
Surface Morphology & PSD



Blank PLGA NPs

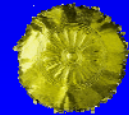


PLGA NPs Loaded with OVA & MPLA





PLGA NPs Loaded with OVA & MPLA

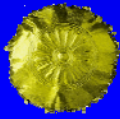


Sample	Av. Diam. (nm)	Zeta potential (mV)	OVA loading (%wt)	MPLA loading (%wt)
DE-RG752H-OVA-MPLA-002	338	-15.7	9.17	0.182
DE-RG752H-OVA-MPLA-003	381	-11.7	10.25	0.165
DE-RG752H-OVA-MPLA-004	444	-14.3	3.11	0.187
DE-RG752H-OVA-MPLA-011	325	-22.3	1.07	0.177
DE-RG752H-OVA-MPLA-007	416	-18.2	9.29	0.909
DE-RG752H-OVA-MPLA-005	341	-16.7	2.97	0.809
DE-RG752H-OVA-MPLA-006	329	-25.2	0.82	0.640
DE-RG752H-OVA-MPLA-009	304	-20.0	0.106	0.798
DE-RG752H-OVA-MPLA-012b	296	-23.2	1.42	1.081
DE-RG752H-OVA-MPLA-012c	294	-27.0	1.456	0.952
DE-RG752H-OVA-MPLA-010	303	-21.6	0.116	1.75

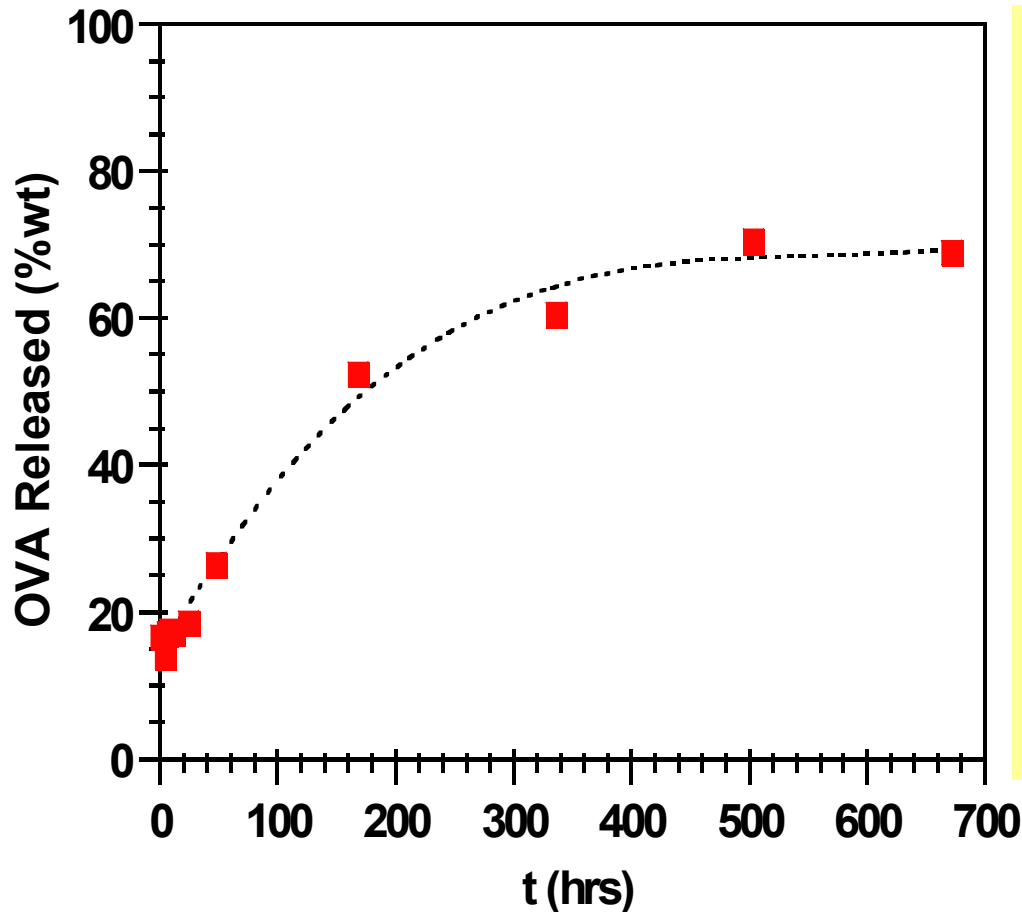
- ✓ OVA loading: 0.1 - 10 %wt
- ✓ MPLA loading: 0.16 - 1.75 %wt



OVA Release Profile



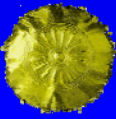
Release profile of OVA from PLGA NPs in PBS at 37°C



- Vials containing 1mg of NPs and 1ml of PBS were incubated at 37°C in a thermomixer at 1400rpm.
- At appropriate time intervals (2, 4, 8, 12, 24, 48, 1wk, 2,3,4wks) 1 ml sample of release medium was collected following centrifugation at 12,500rpm for 10min.
- The amount of OVA released from the NPs in the supernatant was measured by BCA.

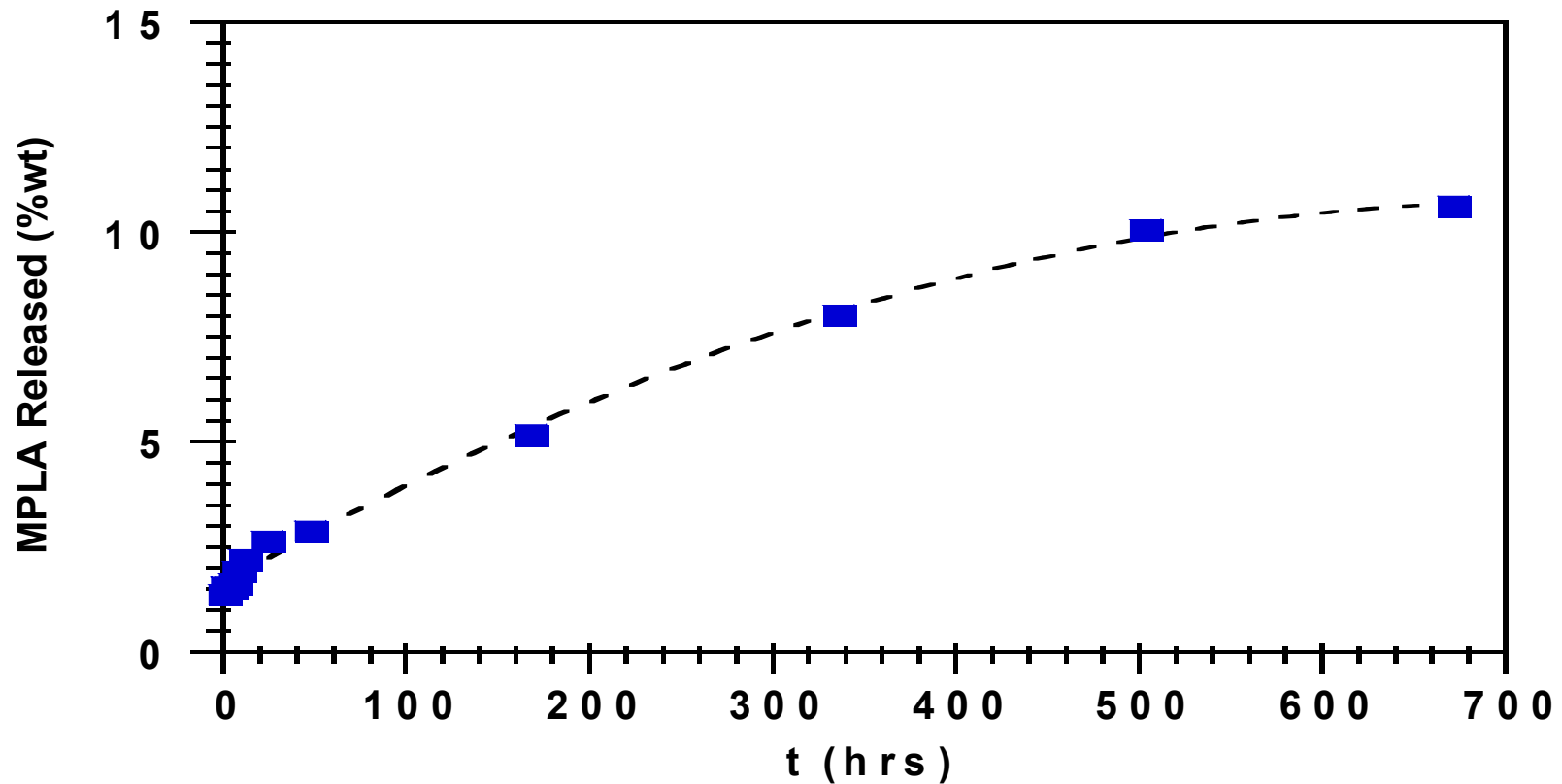


MPLA Release Profile



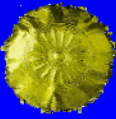
- The amount of MPLA released from the PLGA NPs in the supernatant was measured by LAL.

Release profile of MPLA from PLGA NPs in PBS at 37°C



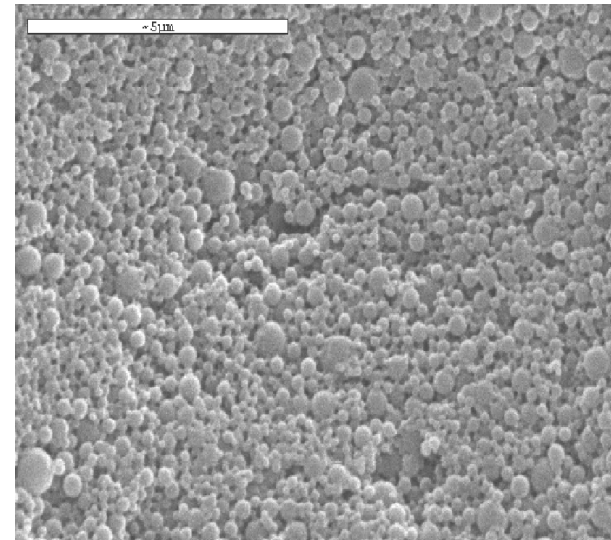
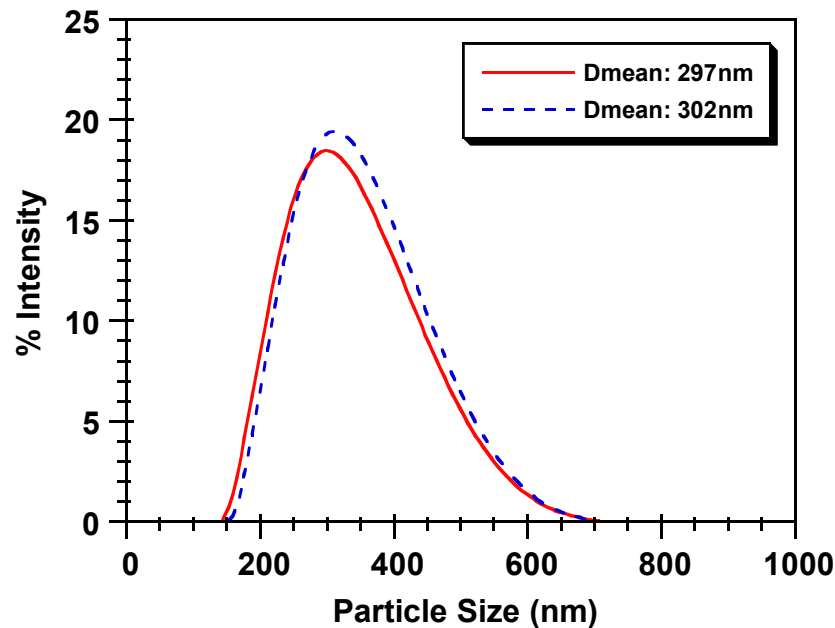


Cell Uptake Studies



- Fluorescently labelled PLGA NPs were prepared for cell uptake studies.

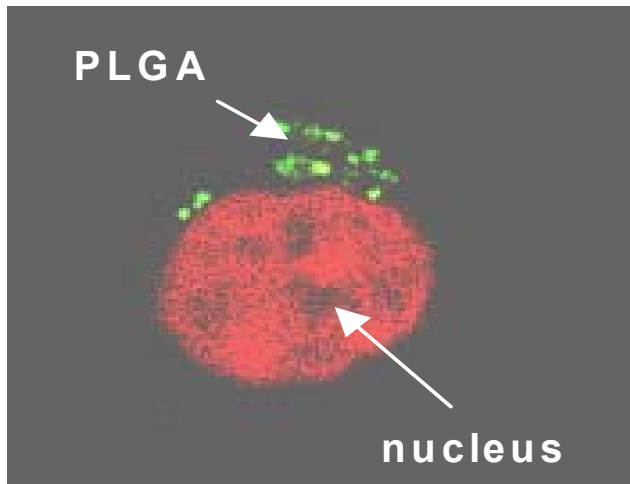
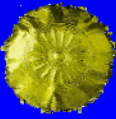
Sample	Av. Diam. (nm)	Zeta potential (mV)	BSA-FITC loading (%wt)
DE-PLGA-BSA-FITC-001	297	-11.8	4.58
DE-PLGA-BSA-FITC-002	302	-10.53	5.10
DE-PLGA-BSA-FITC-003	289	-9.91	5.64



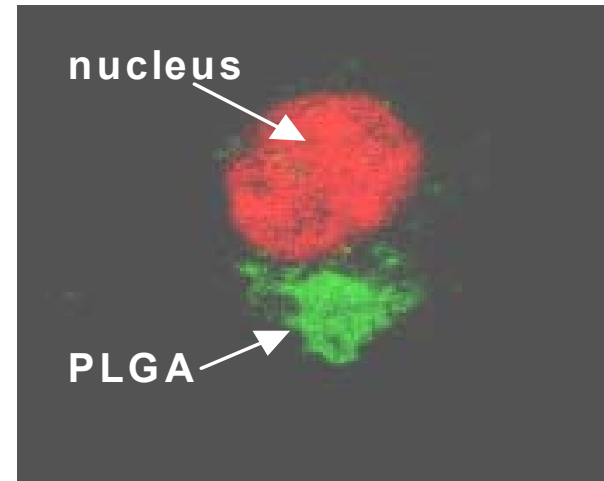
- ✓ The NPs were reported to be non-cytotoxic (MTS & LDH release assays).



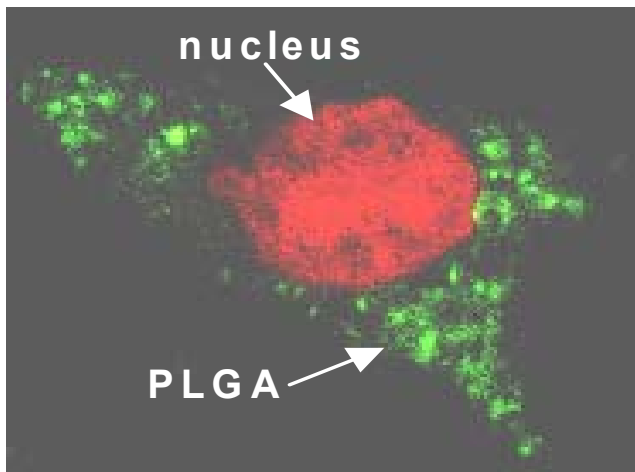
Cell Uptake



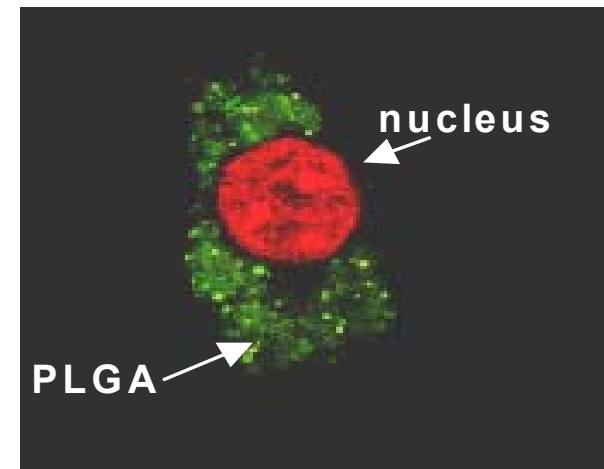
15min



1hr



6 hrs

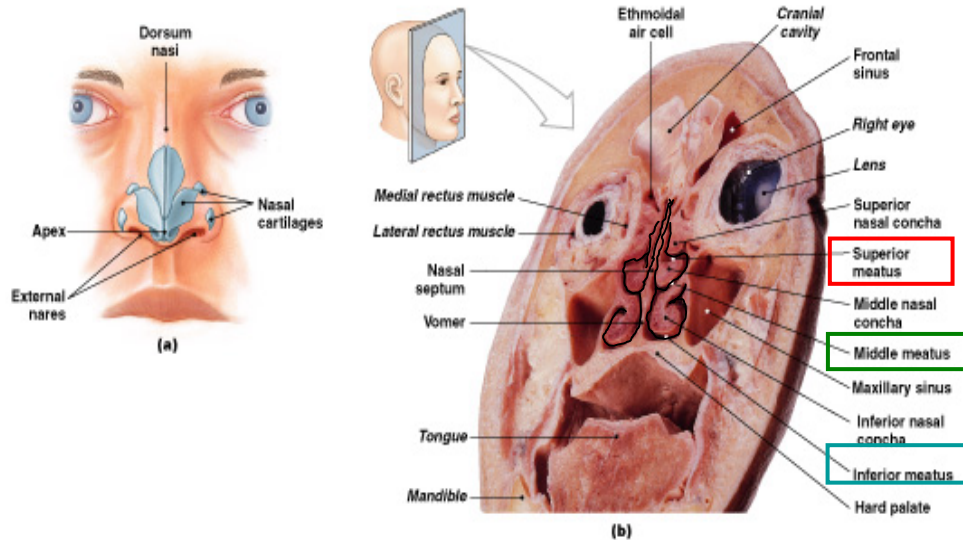
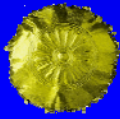


24hrs

Cell uptake of BSA-FITC loaded PLGA NPs (cell line J774)



Geometry of Nasal Cavity



Nasal cavity geometry and symmetry differs significantly between people (more so than other physiological structures of the pulmonary system).

Length of Nasal Cavity: 10-11cm:

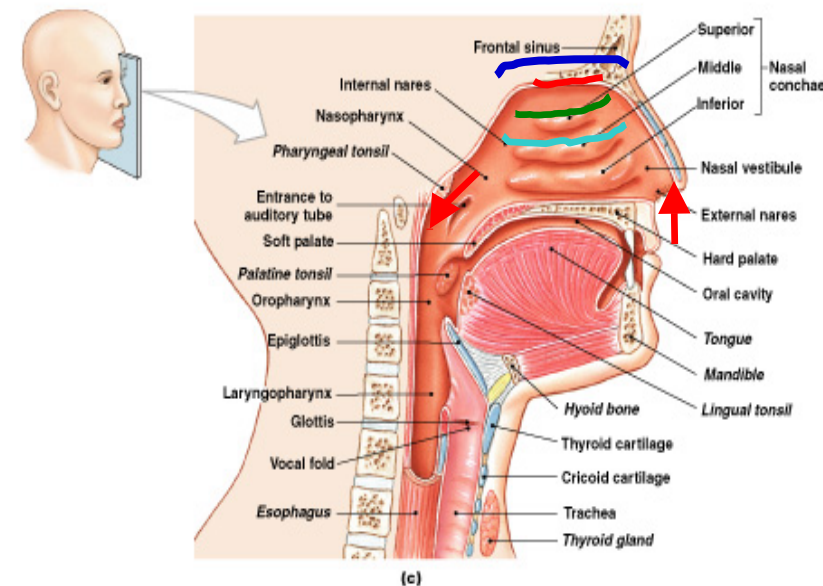
Airflow: 15-25 l/min

Mucosal transport velocity: 5mm/min

Air flows into the nasal cavity through the nostrils undergoing a 70-90° turn into the nasal valve region. Three nasal conchae separate the nasal cavity into three regions, namely, **superior, middle and inferior meatus.**

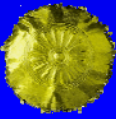
The olfactory region is situated above the superior turbinate.

The structures converge again to the nasopharynx at the end of the nasal cavity from which airflow is directed to the outlet (pharynx).





Geometry of Nasal Cavity



➤ Construction of Nasal Cavity Geometry

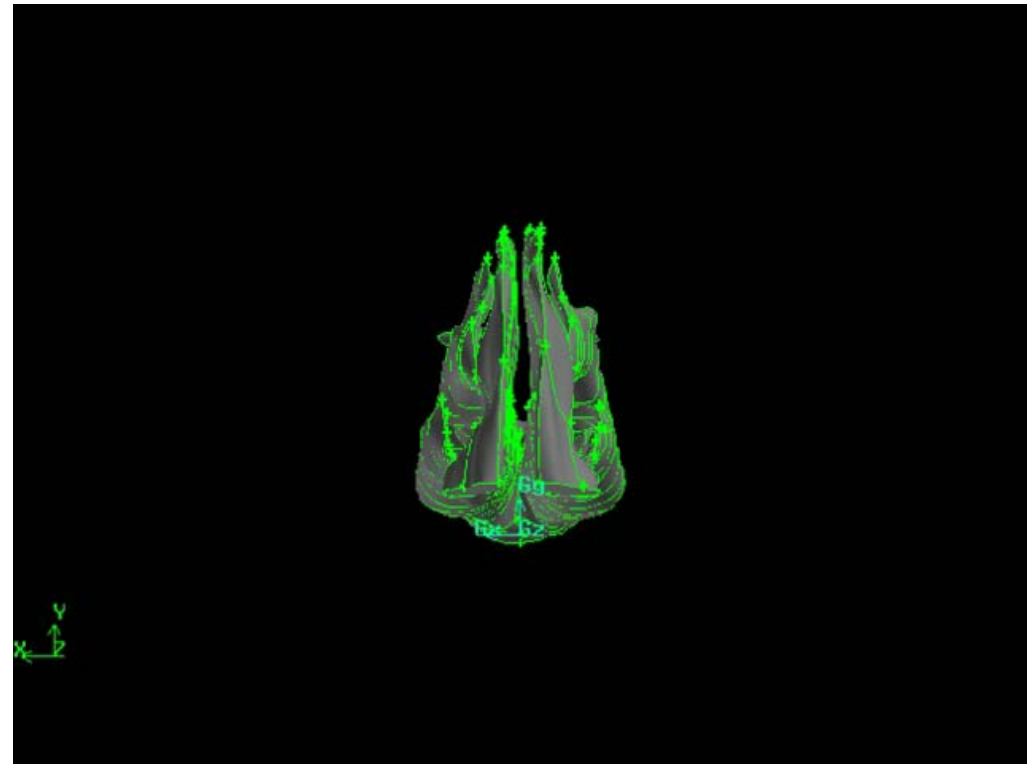
- ✓ Digital data (e.g., with CT or MRI)
- ✓ In general 10-20 slices separated by 1 to 5mm are required to resolve the complex nasal cavity geometry
- ✓ Geometry nasal cavity obtained from Shi et al. (2008)

➤ CAD/CAM

- ✓ GAMBIT (FLUENT)
- ✓ ICEM (FLUENT)
- ✓ FIDAP (FED)

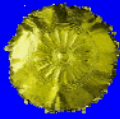
➤ Software

- ✓ AMIRA
- ✓ Flo Works

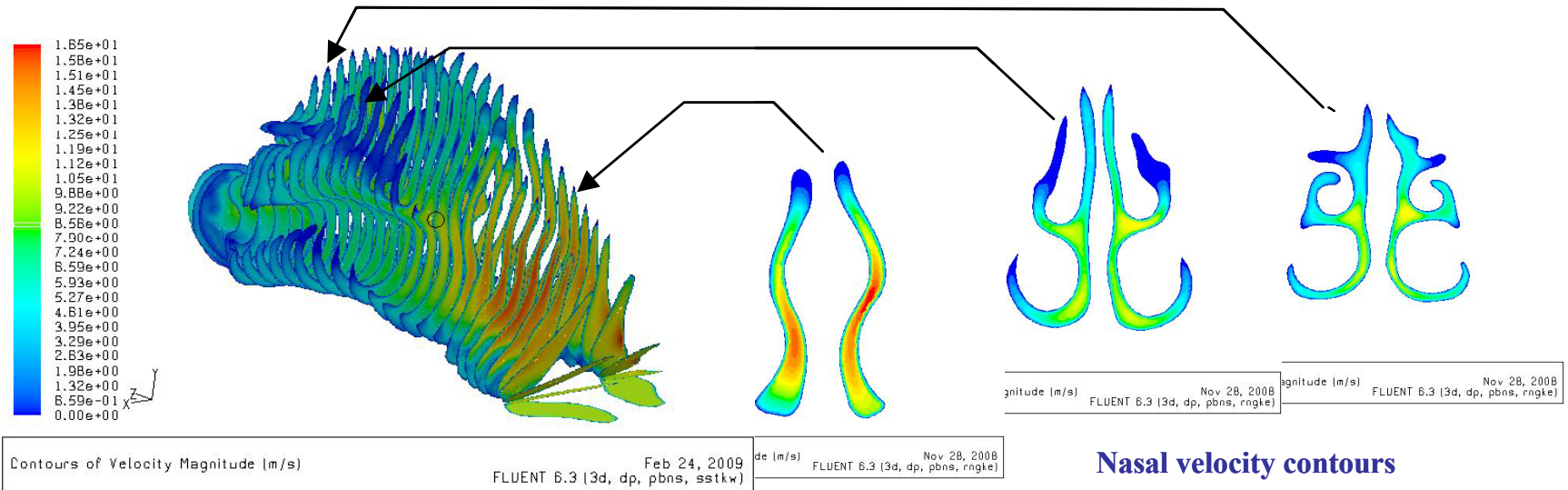




CFD Results: Velocity Contours



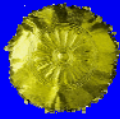
- Simulations were performed for different inlet velocity magnitudes, profiles, and directions, different outlet conditions, different inlet turbulent intensities as well as different viscous models (e.g., laminar, k- ϵ , RNG k- ϵ , k- ω)



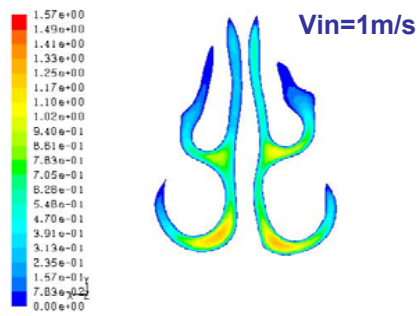
- The flow varies from laminar to turbulent. For inflow velocities $v_{in}=1-2\text{m/s}$ (typical of regular breathing) we have $Re=900-1800$, respectively.
- The flow is strongly non-homogeneous. Largest velocity magnitudes occur in the region near the nasal valve. Flow is directed towards the regions where the nasal cavity meatuses intersect.
- Only limited flow reaches the outer tips of the meatuses and the olfactory region.



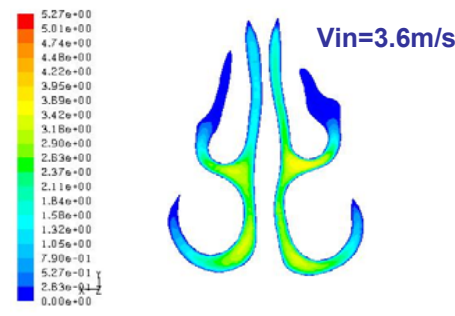
CFD Results: Velocity Contours



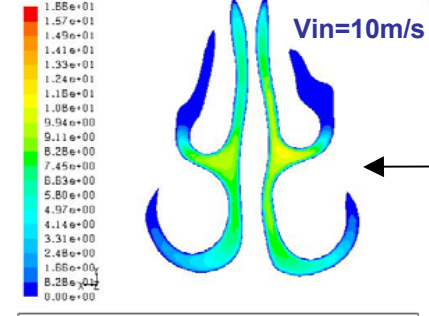
➤ Effect of velocity magnitude



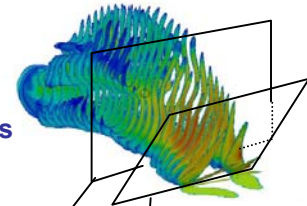
Contours of Velocity Magnitude (m/s) Nov 30, 2008
FLUENT 6.3 (3d, dp, pbns, ske)



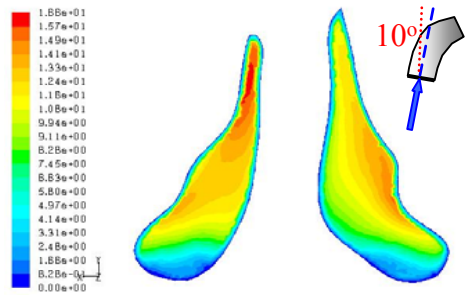
Contours of Velocity Magnitude (m/s) Nov 28, 2008
FLUENT 6.3 (3d, dp, pbns, rangle)



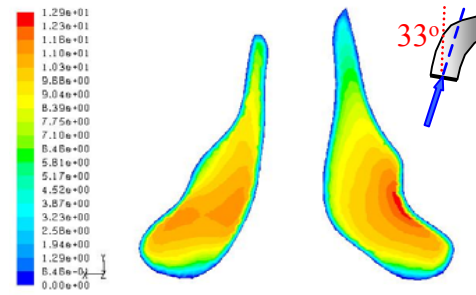
Contours of Velocity Magnitude (m/s) Nov 30, 2008
FLUENT 6.3 (3d, dp, pbns, ske)



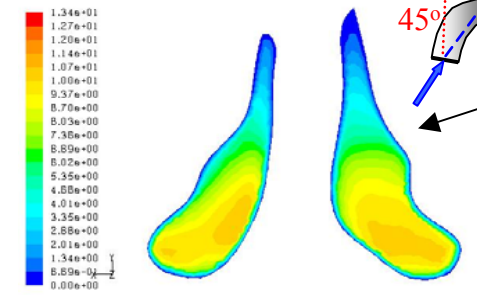
➤ Effect of inlet velocity angle (θ = is the angle between the direction of inlet and the direction of y-axis).



Contours of Velocity Magnitude (m/s) Dec 01, 2008
FLUENT 6.3 (3d, dp, pbns, ske)



Contours of Velocity Magnitude (m/s) Dec 01, 2008
FLUENT 6.3 (3d, dp, pbns, rangle)

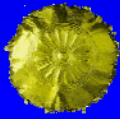


Contours of Velocity Magnitude (m/s) Dec 01, 2008
FLUENT 6.3 (3d, dp, pbns, rangle)

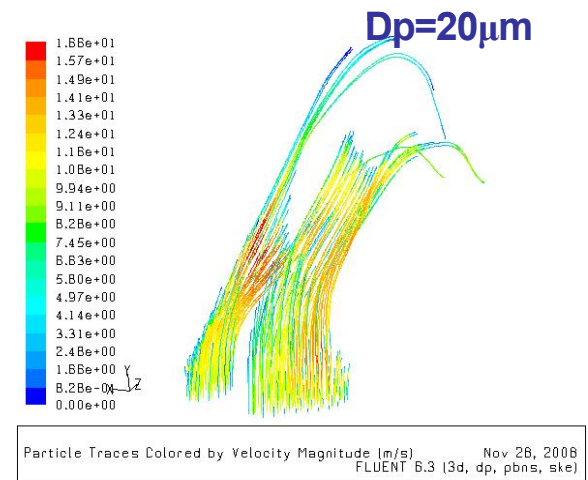
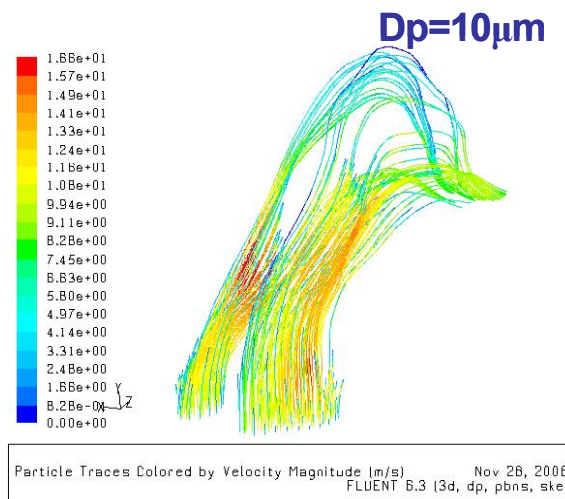
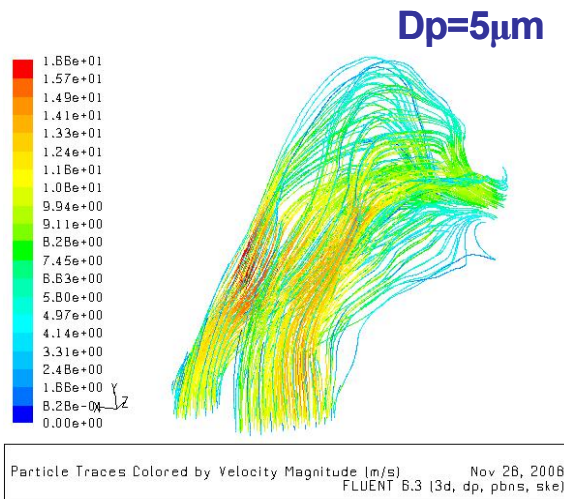
Large inlet velocity magnitudes direct the flow towards the middle meatus intersection. Inlet velocity angle affects the profiles only in the interior region of the nasal cavity.



Particle Streamlines



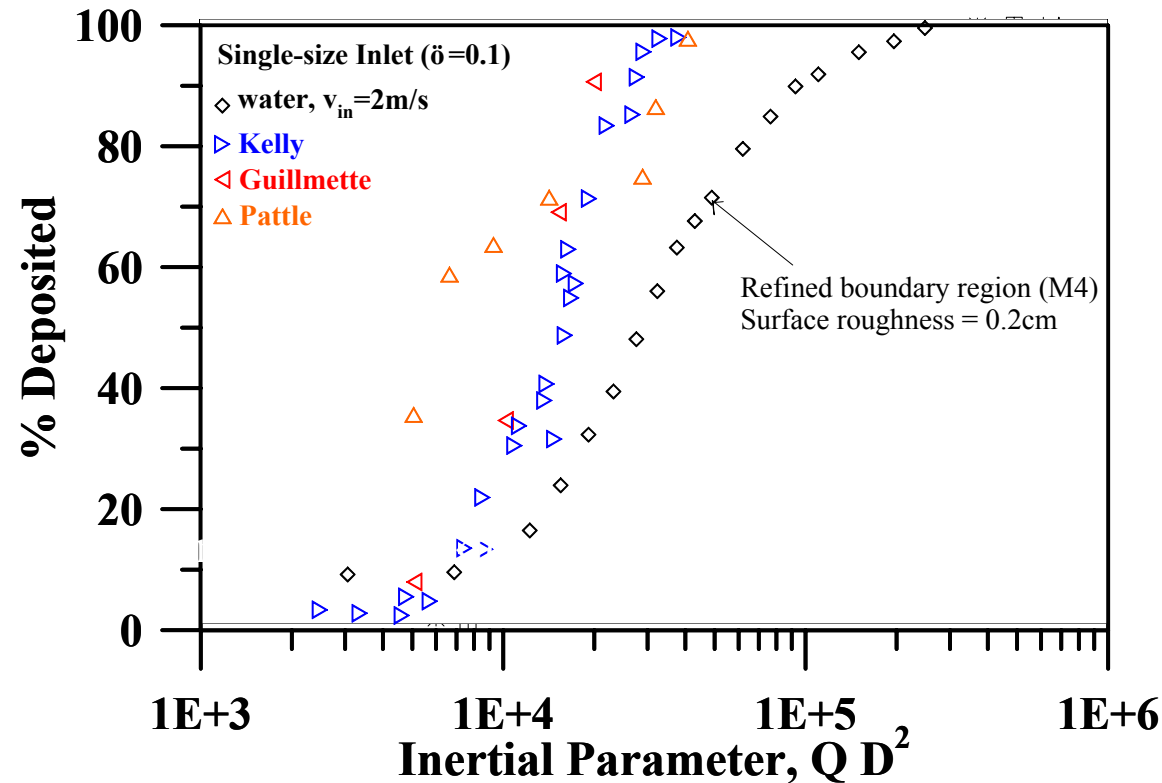
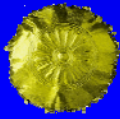
- Particle tracking was performed based on a CFD solution for fluid flow.
- Inertial forces dominate the deposition process of micron sized particles in the nasal cavity. Deposition of smaller (i.e., $<1\mu\text{m}$) particles is much smaller.
- Turbulent dispersion and surface roughness increased particles deposition.



- Increasing particle size increases the total deposition fraction and also decreases the average axial deposition distance from the nostrils (i.e., z_d).



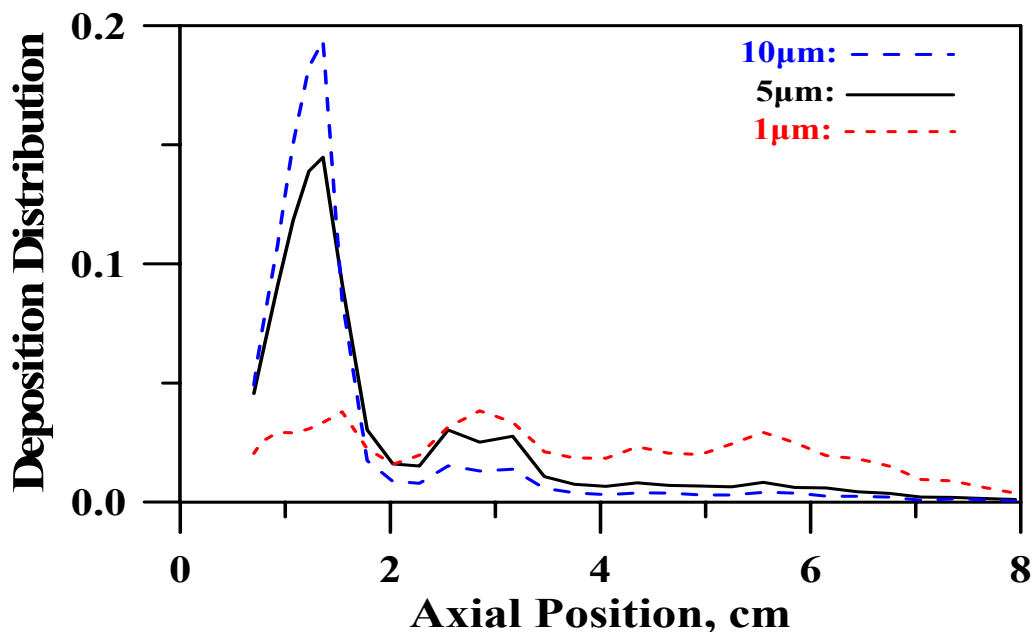
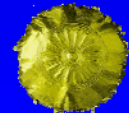
Fractional Deposition In The Nasal Cavity



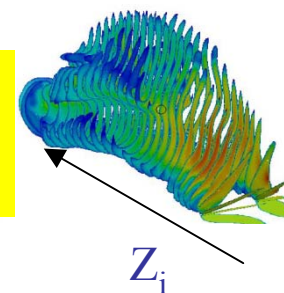
- Comparison of CFD results with experimental data (corresponding to different geometries).
- Results for different particle sizes, D , and inlet velocities, v_{in} , lie on in the same curve in terms of % deposition vs. impact factor, QD^2 , where $Q = A v_{in}$.
- Both surface roughness and turbulent dispersion increased particle deposition.



Particle Deposition Distribution



Deposition distribution, N_i :
Number of particles which deposit between Z_i and Z_{i+1} .



- The fractional particle deposition increased with particle size and inlet velocity.
- Average axial deposition length, z_d , decreased with particle size.
- Large particles ($\sim 10\mu\text{m}$) deposit strongly in the anterior region of the nasal cavity.
- Small particles ($\sim 1\mu\text{m}$) deposit more evenly throughout the length of the nasal cavity.

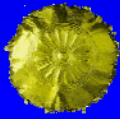
Diameter, μm	Captured, %	Mean Axial Deposition, cm
1	4.6	~ 5.5
2	7.1	~ 4.5
5	19.6	3.6
10	74.6	2.4
15	99.9	1.9
20	100	1.5

model k- ϵ , uniform diameter, $v_{in}=10\text{m/s}$

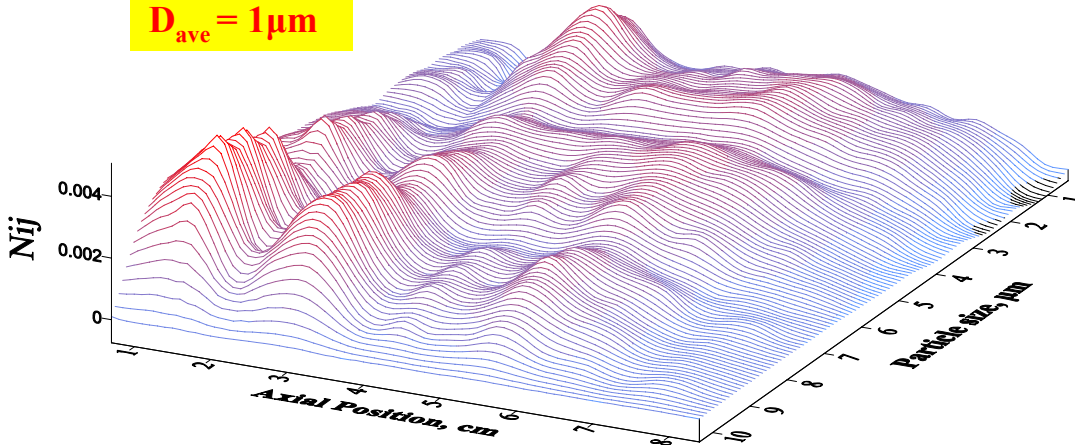
k- ω model, $V_{in}=10\text{m/s}$, zero turbulent dispersion and zero roughness
Rosin-Rammler distribution
Dispersion parameter = 3.5, mean size = 1 and $10\mu\text{m}$



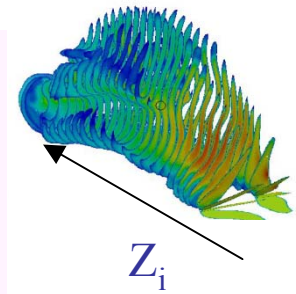
Bivariate Deposition Distribution



$D_{ave} = 1\mu m$

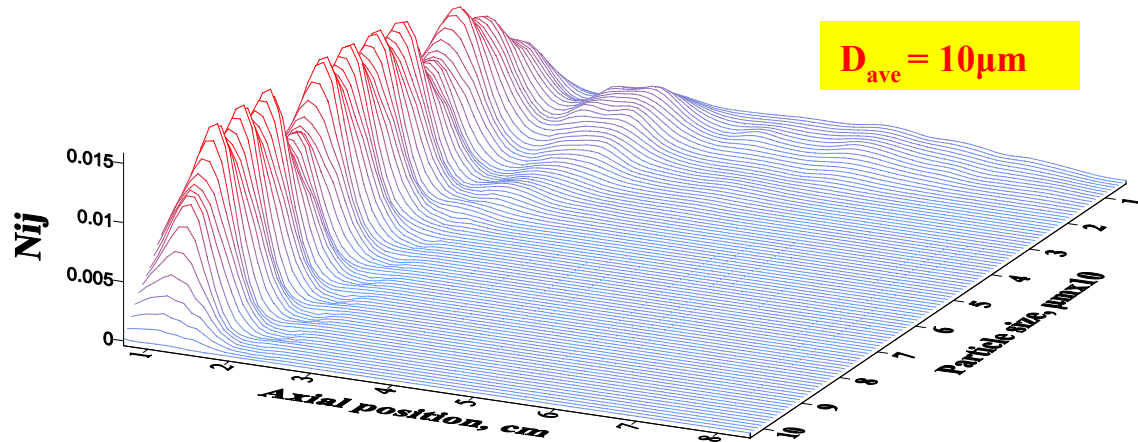


Bivariate deposition distribution, N_{ij} :
 Number of particles in the size range $[D_j, D_{j+1}]$ which deposited between Z_i and Z_{i+1} .



k- ω model
 zero turbulent dispersion and zero roughness
 Rosin-Rammler distribution,
 $V_{in}=10m/s$ inlet velocity
 Rosin Rammler distribution
 Dispersion parameter =3.5
 Mean Size = 1 and 10 μm
 Mean Axial Deposition
 10 μm : 1.44cm
 1 μm : 3.23cm

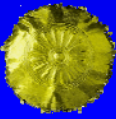
$D_{ave} = 10\mu m$



➤ Small particles (i.e., 1 μm) deposit less than large particles (i.e., 10 μm) but their deposition is much more uniform.



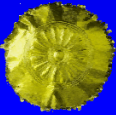
Future Challenges



- Development of synthetic nanometer sized delivery systems for therapeutic agents of increased complexity, able to tackle challenging diseases:
 - ✓ Targeted delivery schemes that accumulate the therapeutic agent specifically on the diseased cells for **cancer** treatment.
 - ✓ Targeted agents able to deliver a drug that stabilizes the **atheromatic plaque** and prevents rupturing.
 - ✓ Delivery of NPs that selectively attach to stem cell niches and release local stimulating factors for the treatment of **musculoskeletal disorders**.
 - ✓ Nanocarriers with special surface properties able to cross the blood-brain-barrier (BBB) for the treatment of **neurodegenerative diseases**.
 - ✓ Non-parenteral formulations of NPs containing insulin.



Acknowledgements



Many thanks to

- to you for your attention,
- to my research associates for their contributions:
 - Dr. Olga Kammona
 - Dr. Vassilis Karageorgiou
 - Dr. Aleck Alexopoulos
 - Dr. Katerina Kotti
 - Dr. Olympia Kotrotsiou
 - Dr. Sotiria Chaitidou
- to EU and GSRT for their financial support.